International Journal of Engineering & Technology, 7 (4.13) (2018) 43-52

SPC

International Journal of Engineering & Technology

Website: www.sciencepubco.com/index.php/IJET

Research paper

Heat transfer performance of multiple holes impingement cooling technique

M F Mohd Zulkeple[1], A R Abu Talib[1,2*], E Gires[1], M T Hameed Sultan[2], M S Ramli[1]

[1]*Aerodynamic, Heat Transfer & Propulsion Group (AHTP), Department of Aerospace Engineering, Universiti Putra Malaysia, 43400 Serdang, Selangor, Malaysia*
[2]*Aerospace Malaysia Research Centre (AMRC), Faculty of Engineering, Universiti Putra Malaysia, 43400 Serdang, Selangor, Malaysia*
**Corresponding author E-mail: abdrahim@upm.edu.my*

Abstract

This research presents the possibility of the jet impingement cooling technique configuration for stator of turbine blade under the transient heat transfer condition. The main goal of this study is to investigate the impingement cooling plate holes configuration and Reynolds number (*Re*) effect on the heat transfer which can be observed from the color play of the thermochromic liquid crystal (TLC). The findings proved that with the present of the small holes in between the main larger holes capable to enhance the heat transfer across the target surface. However, some criteria of the design need to be taken into count as it may produce different heat transfer performance of the impingement cooling technique. Therefore, in the range of predetermined design parameters, only several combinations that prevailed to achieve maximum heat transfer across the target plate.

Keywords: *liquid crystal; impingement cooling; heat transfer.*

1. Introduction

Jet impingement is a technique that cools the inner surface of the blade through the tiny holes in the impingement insert. It is a very efficient technique for the first stage vane of blade. This is because cooling air can be directly delivered to impinge the hot regions surface. But the present of cross flow may disturb the flow of impinge air which reduce the cooling effect on the hot regions. To be best among other cooling technique does not come without drawback. The installation of this technique must be made with a detail consideration due to its construction that may weaken the structural strength of the turbine blade. Therefore, this technique usually been placed only at the region where the temperatures rise is large which usually at the leading edge of the blade as shown in Figure 1.

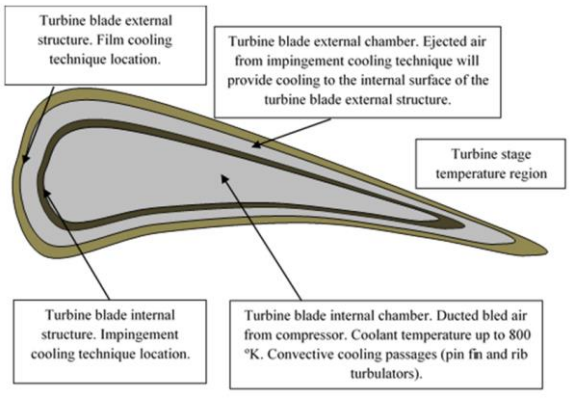


Fig. 1: Placement of impingement cooling technique [1]

The mechanism of the jet impingement cooling technique involves the ejection of air flow through the hole to hit or impinge the targeted surface. The application on the real gas turbine is usually in the form of multiple impingement jet holes rather than single jet hole which to cover more area of the targeted surface. Generally, turbine blade is divided into two compartments. The first compartment is the compartment that been pressurized by having higher pressure than the other. The impingement air discharge will increase as the pressure gradient rise. The second compartment is the compartment that will then experience the impingement effect due to this pressure gradient. The design and application of this impingement technique may be simple to make it on the top in term of efficiency to improve the heat transfer coefficient, but the heat transfer analysis become savage when involving the interaction between the neighboring jet holes air flows.

Shape of the holes of the jet can affect the rate of heat transfer. This is since the shape of the holes could affect the rate of the mass flow through it. Some researcher has done a detail experiment to study on the effect of the holes shapes on the heat transfer. According to the research has been done by Ndao *et al*. [2], which involve testing of four different shapes of jet holes. From the result obtained, the coefficient of heat transfer for circular and square shape is higher compare to elliptical and hydrofoil shape holes. This could be due to the present of the secondary flow.

The configuration of impingement hole can affect the rate of heat transfer between the fluid and the targeted surface. For hole arrangements, there are some investigation that been done to compare the heat transfer rate for inline and staged arrays of the holes. According to Fechter *et al*. [3], inline array of holes has larger coverage of the targeted surface which able to provide higher average heat transfer coefficient. Experimentally, staggered hole has

Copyright © 2018 Authors. This is an open access article distributed under the Creative Commons Attribution License, which permits unrestricted use, distribution, and reproduction in any medium, provided the original work is properly cited.

lower of heat transfer coefficient on the target plate compere to inline hole which showing there is some reduction on the rate of heat transferred to the plate. In another paper, Liao *et al*. [4] stated that the rate of heat transfer is reduced as the holes offset become further from the channel centerline. On the other hand, Hollworth & Dagan [5] state that staged arrangement is better to increase the heat transfer compare to inline arrangement especially at smaller jet to target distance. But then Liu *et al*. [6] state that as the distance between the jet and the target is increases, the cross-flow coverage will become larger. This will absolutely affect the rate of heat transfer of the jet.

The heat transfer of the impingement technique can be further optimized by varying the diameter of the jet holes. According to Singh *et al*. [7] the effect of the jet diameter on the heat transferred can be observed from two points of view which are local Nusselt number (*Nu*) and Stagnation *Nu*. For constant jet–to-plate spacing and *Re*, small diameter jet produces higher velocity flow, but lower mass flow rate compares to bigger jet diameter. Due to the higher velocity of the flow, the stagnation point *Nu* is higher, but the local *Nu* is lower compared to larger diameter jet size. This is because of the mass flow rate of the smaller jet diameter is lower compared to larger diameter. Other research that been done by Yang *et al*. [8] that using Computational Fluid dynamic software to simulate that temperature contour of the impingement fluid. It is obvious that, the stagnation point of the flow is always occurring in the center of the flow. This outcome leads to the same conclusion as Singh *et al*. [7].

Generally, the main objective of the project was to investigate the impingement cooling plate hole configuration effect on the heat transfer that can be observe from the color pattern of the thermochromic liquid crystal (TLC). The method that involved in this study was consists of fabrication of the designed plate which have different holes configuration, run the cold and hot test and finally the analyzing of the obtained result. The expected result from this study was that, with the present of small holes between the main big holes will enhance more heat transferred across the plate in addition to a staged configuration that also predicted will propagate the level of heat transfer across the plate surface. This is because, with the present of small holes it will contribute to stagnation heat transfer while big holes will contribute to higher jet wall heat transfer coefficient. Besides that, it also expected that at higher *Re*, rate of heat transferred is also high across the plate surface for all test plate.

2. Methodology

The design of the experiment facility, which was the wind tunnel was referred to British Standard 1981, BS1042: Measurement of fluid flow in closed conduit [9] as shown in Figure 2. The purpose of the designed experiment facility was solely for research of the gas turbine impingement cooling technique. The temperature was measured based on the observation of the thermochromic liquid crystal (TLC) color play on the target plate and fast response T-type thermocouple data which gained from the data acquisition system. The TLC was calibrated first before been used in the experiment using the method stated by Abdullah *et al*. [10]. The result acquired from the color changes of the TLC were captured by digital video camera. The observation from the video was extracted into frames before been further processed. The experiment test for the impingement plate involves two methods of testing which were cold and hot testing.

The conduit in this experiment was a straight cylindrical passage of constant cross-section area and had the length of that long enough to ensure that the upstream flow of the air was fully developed and swirling free before reached the orifice part. The cross-section of the conduit must be between the ranges of 0.05 m to 1.20 m and the *Re* higher than 3150, otherwise the equation used become invalid. Most of the devices on the conduit were depending on the pressure differences which were the difference of static pressure between the upstream and downstream section values. The pressure difference from the wall pressure tapings on the conduit were used to calculate the mass flow. The orifice that act as the controller for the mass flow of the air was also been designed according to BS1042.

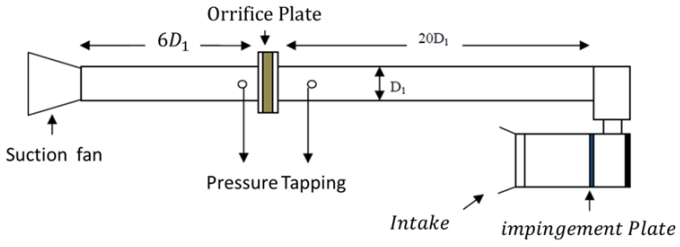


Fig. 2: Sketch of the conduit used for the experiment

For the design of the intake nozzle, the type that was selected for this study was based on ISA1932 which direct the fluid into the test region in an appropriate manner. The intake nozzle was placed on the front section of the test region which about 20 mm before the hot mesh grid.

The fast response mesh heater which will heat up the air flow during the transient test was constructed to have two sections which allow the mesh heater to be held by the rig. The length of the mesh heater was designed to be a bit logger and the smaller mesh wire diameter so that the air flow can be fully been heat up. The terminal was made from the copper material because copper higher electric conductivity compared to the brass material that been used in original design. This will allow the speed of the air been heated become faster. The usage of the wood and mica material combination for the body the mesh heater will provide thermal protection and high electric resistivity.

The installation of the orifice on the conduit will increased the kinetic energy and drop the static pressure in the same time due to the downsizing of the cross-sectional area of the gas flow path. These pressure changes will be used later for the calculation of the mass flow rate of the gas.

2.1. Impingement plate design

There was a total of five plates that were used in the experimental work. These plates were designed to represent the different impingement jet holes configuration with and without the present of smaller holes in between which were arranged in form of inline and staged array. Each impingement plate had the main holes diameter of 10 mm while the smaller holes diameter was 5 mm with the thickness of 12 mm. Figure 3 illustrated the drawing of the inline holes configuration with (Plate A) and without (Plate B) the small holes plate while Figure 4 illustrated the drawing of the staged holes configuration with (Plate C and Plate D) and without (Plate E) small holes plate.

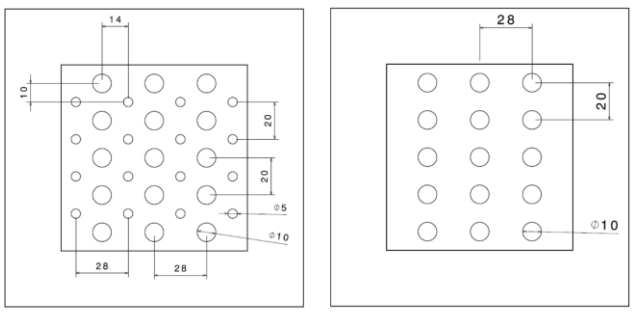


Fig. 3: Drawing of the inline holes configuration plate.

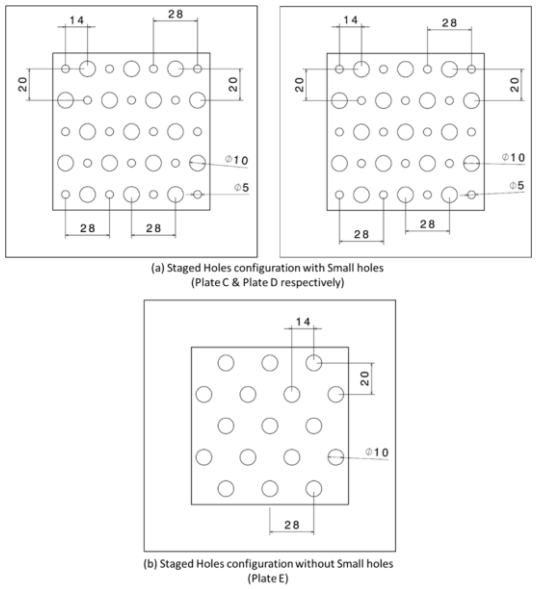


Fig. 4: Drawing of the staged holes configuration plate.

The smaller hole was design so that it provided a high velocity air passing through the holes that was mentioned by Singh *et al*. (2013), which stated that the effect of holes diameter can be observed from two point of view which are local and stagnation heat transfer. Due to higher air velocity of flow, the stagnation heat transfer for smaller hole was higher compared to bigger holes. This will enhance the heat transfer across the plate. The bigger hole design was based on the what have been mention by Ramli *et al*. (2016) which state that big hole provides more opening to allow air to pass through which mean that more air was impinged the surface which contribute to higher local heat transfer. With this both finding, both small and big holes been combined to enhance the heat transfer across the surface to the higher level.

The material of the impingement plates was Perspex (acrylic glass) material because acrylic has low thermal diffusivity characteristic which assumption of the one-dimensional semi-infinite heat transfer become more valid for the experiment [12]. The fabrication of the plates was being done using Computer Numerical Control (CNC) machines.

Furthermore, the surface temperature response was only valid for a thin layer on the surface and no lateral conduction occurs. This mean that the time for the experiment to be run must be determined as to prevent the occurrence of lateral conduction on the surface. The governing equation for the time limit of the experiment given by Mohd Saiah [1] was:

$$t = (x/4)^2/\propto \quad (1)$$

where t was the experiment time limit, x represented the penetration depth and ∝ was the thermal diffusivity of the test subject.

For this study, unsealed liquid crystal been used, and the microencapsulation process was performed separately to utilize the user-defined formulation. The term microencapsulate was defined as a small substance been surrounded by uniform walls. The microencapsulation process utilizes uniform continuous polymer coatings around the wall of the liquid crystal to form an individual crystal shape on the surface. This process was to provide isolation to the liquid crystal from been affected by the surrounding due to the polymer coating and make the crystal to be in the form that practically easy to use [13]. The mixture between liquid crystals, aqueous binder and water used for the microencapsulation process were performed with ratio of 5:1:6 as stated by Abdullah *et al*. [14]. All these substances were mixed together according to the ratio in a small container and been shaking to allow the microencapsulation process to occur until the mixture achieves a smooth milky color without any visible gel shape substance.

2.2. Experimental setup and procedures

2.2.1. Cold test

The cold test was done to determine the *Re* which will be used to investigate the effect of flow *Re* on the heat transfer coefficient. The calculation of *Re* value can be obtained using Eqn. 2.

$$Re = \rho VL/\mu \quad (2)$$

In which *Re* = Reynolds Number (non-dimensional), V = velocity of the fluid (ms^{-1}), L = length or diameter of the fluid (m), μ = viscosity of the fluid (for air:1.983×10^{-5}) kg/ms).

Before calculating the *Re*, the velocity of the air should be determined first which can be obtained from the mass flow rates that pass through the orifice that been equipped with pressure tapping (Figure 5).

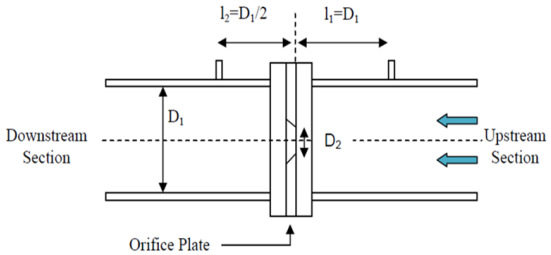


Fig. 5: Orifice with pressure tapping [1]

Based on orifice in Figure 5, the Bernoulli's equation between the two-pressure point can be written by assuming the flow to be steady, in viscid and incompressible flow which lead to Eqn. 3,

$$P_1 + 0.5\,\rho V_1^2 + \rho g h_1 = P_2 + 0.5\,\rho V_2^2 + \rho g h_2 \quad (3)$$

Since point 1 and point 2 was at the same level, the value of h_1 and h_2 was same, therefore, $\rho g h_1$ and $\rho g h_2$ which simplified the equation to be,

$$P_1 + 0.5\,\rho V_1^2 = P_2 + 0.5\,\rho V_2^2 \quad (4)$$

By rearranging the equation and substitutingP_1-P_2=ΔP, the equation then become,

$$\Delta P/\rho = (V_1^2 - V_2^2)/2 \quad (5)$$

The velocity term can be expressed in term of flow rate (q_m), Cross-sectional area (A), and density ((ρ);

$$V = q_m / A\rho \quad (6)$$

By substitute Equation 6 into equation 5, the equation will become

$$\Delta P/\rho = 0.5\,[(q_{V2}^2)/(A_2^2\,\rho^2) - (q_{V1}^2)/(A_1^2\,\rho^2)] \quad (7)$$

The equation then been further simplified by applying the continuity theory which state that q_V=q_{V1}=q_{V2}, and make the equation to become,

$$\Delta P/\rho = (q_V^2)/(2\rho^2)\,[1/(A_2^2) - 1/(A_1^2)] \quad (8)$$

The equation was being rearrange again to form an equation of flow rate in term of pressure difference, area and density and bear in mind that β=D_2/D_1

$$q_V = \sqrt{(2\rho\Delta P / [1/(A_2^2) - 1/(A_1^2)])} = A_2\sqrt{(2\rho\Delta P / [1-(A_2^2)/(A_1^2)])}$$

$$q_V = A_2\sqrt{(2\rho\Delta P / [1-\beta^4])} \quad (9)$$

where $A_2/A_1 = (2\pi D_2^2)/(2\pi D_1^2) = (D_2^2)/(D_1^2) = \beta^2$

In Eqn. 9, q_V was the mass flow rate in the pipe on the orifice region where there were no losses due to the frictional effect been considered. Therefore, the discharge coefficient, C can be introduced to equation 9 to take count these losses for the calculation of the actual flow rate of in the conduit.

$$q_V = CA_2\sqrt{(2\rho\Delta P / [1-\beta^4])} \quad (10)$$

By referring to BS1042, the governing equation of the discharge coefficient was given to be,

$$C=0.5959 + 0.0312\beta^{2.1} - 0.184\beta^{8} + 0.0029\beta^{2.5} [10^{6} / Re]^{0.75} + 0.09L_1 \beta^{4} (1 -\beta^{4})^{-1} - 0.0337L_2 \beta^{3}$$

where C was the discharge coefficient, β was the diameter ratio, *Re* is the Reynolds Number and L_1 was the ratio of l_1 / D_1, L_2 was a ratio of l_2/D_2. BS1042 also state that, whenever $L_1 > 0.039/0.090$, 0.039 will be used for the term $\beta^4 (1 -\beta^4)^{-1}$. Since in this study $L_1=1$, the discharge coefficient equation become,

$$C = 0.5959 + 0.0312\beta^{2.1} - 0.184\beta^{8} + 0.0029\beta^{2.5} [10^{6} / Re]^{0.75} + 0.00351L_1 - 0.0337L_2 \beta^{3}$$

The value of the discharge coefficient, C can be obtained from the iteration process because *Re* was needed to calculate it. Therefore, initial guess of the *Re* been taken to get the value. However, the *Re* that been used in the iteration process cannot be used to get the velocity to calculate the *Re* of the conduit which need the value of C first.

Basically, the cold test been done by varying the diameter of the orifice hole. Before starting the cold test, there was a setup that must be done which is the digital manometer must be connected to the pressure tap using small air tube to measure the pressure different. the cold test been done with varying the diameter of the orifice hole and the suction fan power for 3 different condition which is for the condition of no impingement plate, plate 1, plate 2 and finally plate 3. All the pressure different will be recorded based on the manometer reading. This pressure different will be act as the input for the MATLAB coding.

2.2.2. Calibration of TLC

The calibration of the TLC was done by spying the TLC on the surface of the calibration plate that were applied with flat black paint on the top of the plate surface. The purpose of the black surface was to optimize the visibility of the color-temperature response of the TLC. To make a constant environment or condition for the experiment, the same TLC mixture that been used for calibration was applied to target plate on the same day. The target plate that been used was the same material for the impingement plate which was the Perspex. This was because of the high visibility of the materials which allowed the observation of the TLC color played as exposed to the heated air flow.

The calibration of the TLC for the heating process was been done by heat up the air flow which been done by the mesh heater. As the air been heated and been allowed to hit the TLC coated target plate, there will be a color played on the surface. However, the visibility of the color play may not so good, therefore black paint been coated on the target plate to improve the visibility of the color play of the TLC.

Besides that, there also three T-type thermocouples that were used during calibration process. One was placed right after the mesh heater and one was placed just before the impingement plate. This was to make sure that the air flow temperature between the mesh heater and the impingement plate were uniform. The last thermocouple was placed on the surface of the target plate to observe the surface temperature that was used in making the color intensity-temperature relationship history. All three thermocouples were connected to a data logger system which comprised of an AGILENT 34970A Data Acquisition/Switch Unit [15], 20 Channel Multiplexer and a personal desktop computer. The color played by the TLC been recorded using the Video camera.

Some other set up needed for the TLC calibration was the Light-Emitting Diode (L.E.D). This LED acted as the indicator to show when transformer been turned on to heat up the mesh heater. This was to synchronize the video recorded data with the data logger. The LED powered by the power supply was connected to the data logger. The data logger was recording the voltage and the video camera was capturing the moment the LED been turn on. The data logger time step was set up to one second interval which means that the logger was recording the temperature and voltage every one second. The video camera was set to have a better white balance and manual focusing function to have a better quality of the recorded video. To control the light intensity during the calibration process, the rig was covered with thick black cloth and the only light source was from the florescent lamps that were embedded on the rig frame.

The calibration process started with the video camera and the data logger was started at the same time. After about 20 second later, the transformer was turned on to heat up the mesh heater and the LED was turned on to indicate the heating process has started. After about 58 second, the transformed and the LED was turned off to indicate the end of the heating process. From the calibration process, two important data were obtained which was the color play of the TLC that been captured inside the video and the temperature and LED histories that recorded by the data logger.

By using the MATLAB coding that been reproduced based on Abdullah *et al*., [16] algorithm, the data obtained from the calibration process were further processed. The input for this coding were the video of the calibration process that been extracted into 25 frames per second and the temperature and LED histories that been recorded by the data logger. The video was extracted using Adobe Premiere Pro and was named with just alphabetical without any number or symbol because Adobe will extract the video and add a number sequence to the name of the image. From the extracted frames, there should be two important things that must be noted. Firstly, the total number of the extracted frames and the frame number where the LED on indicating the start of the heating process. The product of the calibration process was the 4 relationship which are the intensity against frames number, intensity against times, surface temperature against times and intensity against surface temperature. The relationship of intensity history against the surface temperature was written in the note pad as it will be used as the look-up history to match the color-temperature response of the TLC color play during the transient test.

2.2.3. Hot test

For hot testing, the values that want to find or observe was the heat transfer for each impingement holes configuration. The heat transfer value could be found by observing the color pattern on the surface of TLC.

The setup of the experiment was almost same to calibration setup except the number of the thermocouples that connected to data logger been used were reduced to two which was placed after the mesh heater and just before the impingement plate to ensure the temperature uniformity of the air flow. The only light source was the florescent lamps that embedded just behind the video camera position. The region around the camera and the target plate was covered with black cloth to eliminate other light source except from the florescent lamps. The camera was placed just behind the target plate to record the color plat of the TLC. The positioning of the camera behind the target plate must be adjusted so that there was no reflection of light on the surface of the target plate which will spoil the visualization of color played that been recorded in the video. Besides that, LED that been connected to power supply been stick just beside the target plate within the range of the frame of recorded video to indicate the started and the ended of the heating process.

Before starting the actual transient test, a simple experimental test to observe the temperature uniformity of the air flow pass through the rig has was done. This simple testing only involved the thermocouples that were connected to the data logger. The positioning of the thermocouple was shown in Figure 6.

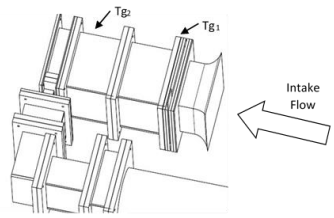


Fig. 6: Positioning of the thermocouple

This simple experiment was conducted with the suction fan speed setting of 50 Hz, the orifice diameter of 20 mm and the current of the transformer was 56 A. The test was started when the suction fan and the data logger were turned on. After 10 seconds, the transformer was turned on. The transformer was turned off as the temperature of the air flow recorded by the data logger has reached the maximum value. The temperature uniformity history of the air flow passed through the rig was shown in Figure 7.

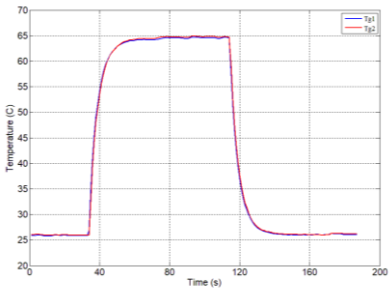


Fig. 7: Temperature uniformity of the air flow

Based on Figure 7, the validation of the transient heat transfer was obtained. The analyzing process of the data for the transient heat test utilized the MATLAB routine reconstructed based on Abdullah *et al*. [16] algorithm. This MATLAB routine deal with one dimensional semi-infinite heat transfer assumption that required the sudden step change on the gas temperature which means that temperature of the gas should rise within 1 second. Therefore, based on the plot, the transient test was valid to use the MATLAB routine reconstruct based on the Abdullah *et al*. [16] algorithm as the mash heater was able to drive heat transfer process and fulfil the assumption that been.

Once the validation been confirmed, the rig was setup for the actual transient heat transfer test which included the positioning of the thermocouple and LED which were connected to the data logger just about 10 mm after the mesh heater and beside the target plate respectively. During the test, the temperature and the voltage were recorded using the Agilent Data logger software. Besides that, the orifice diameter and fan suction power were choose based on the cold test result which was the *Re*. For this study the 20 mm and 30 mm diameter of the orifice and 50 Hz for the fan suction power been choose which have different *Re* based on the cold test result. The video camera been placed behind the target plate and were connected to LCD monitor beside the rig. The video camera was controlled using remote control to avoid any unnecessary disturbance during the test.

As all the set up been done, the suction fan was turned on and been left about 10 minutes to make sure that the flow was steady. While waiting the flow to be stable, all the instruments been checking to confirm that all of them to work the way been desired. As the flow been assumed to be stable, the video camera was started using the remote and the data logger was started at the same time. After 20 minutes, the transformer and the LED were turned on to indicate the heating process has started. By referring to the assumption of the one-dimensional semi-infinite heat transfer, the limit time of test was about 68 second before it become invalid. However, the transformer was offed after 58 seconds because the gas temperature has risen higher that the clearance temperature for the TLC. At the same time the LED was turned off to indicate the end of heating process. The data logger and the video camera were stopped about 20 seconds after the LED off. It is recommended to analyses the first test before processed to the other experiment. The details of the data analysis were further explained on the next sub chapter. If the result from the analysis was good and reliable, the next test with different setup can be conducted.

2.2.4. Data and image processing

The data and images processing were done in personal laptop. The required raw data needed for this processing process were the videos that been recorded that contain the color play of the TLC and the temperature history from the data logger. The videos of the TLC color play will be extracted first into 25 frames per second using Adobe Premiere Pro software. The extracted images were recommended to be named only with alphabet. This was because adobe will add the numeric number according to the sequence of the images in the video. From the extracted frames, the information's that can be harvest are,

a) The frame number which the LED was on.
b) The frame number which the LED was off that also indicating the total number of frames.

Next, the temperature history from the data logger was extracted in form of excel file. From this excel files, the information that going to be needed were:

a) The time interval of the test.
b) The average ambient temperature.
c) The time when the LED was on and the temperature start to climb.
d) the total time of the transient test

All these information that were extracted from the video of TLC color play and the temperature history from the data logger, were act as the input for the MATLAB routine that was developed. With the completing of the image and data processing, the methodologies of the study work are completed.

3. Result and discussion

3.1. Cold test

Table 1 shown the *Re* with its uncertainties for condition where there is no impingement plate been placed. On the other hand, Table 2 to 6 shown the *Re* with its uncertainty for impingement plate A, impingement plate B and impingement plate C, respectively. The calculation of the uncertainty for the *Re* is made up from several sources. Most of the uncertainty is contributed by the pressure different measurement. This is because the manometer that been used for this test has too large range of reading. Basically, it can accurate measure larger pressure different and will become less accurate when dealing with small pressure different. Hence, to achieve elevated level of accuracy of result, only *Re* with uncertainty value below 10 % been used for hot test while higher than 10 % was neglected from consideration.

Table 1: *Re* with uncertainty for without impingement plate condition

Suction Fan Setting (Hz)	Orifice Diameter (m)			
	0.02	0.03	0.04	0.05
	Re			
10	865 ± 57.6 %	1409 ± 115.5 %	2562 ± 115.1 %	null
20	1608 ± 16.5 %	3398 ± 19.3 %	4378 ± 38.4 %	4129 ± 115.1 %
30	2425 ± 7.4 %	4982 ± 9.1 %	7090 ± 14.5 %	8097 ± 28.8 %
40	3260 ± 4.3 %	6467 ± 5.5 %	9346 ± 8.4%	10652 ± 16.5 %
50	4012 ± 3.1 %	8027 ± 3.7 %	11421 ± 5.7 %	13302 ± 10.6 %

Table 2: *Re* with uncertainty for impingement plate A

Suction Fan Setting (Hz)	Orifice Diameter (m)			
	0.02	0.03	0.04	0.05
	Re			
10	865 ± 57.6 %	1409 ± 115.1 %	2562 ± 115.1 %	null
20	1608 ± 16.5 %	3106 ± 23.1 %	4378 ± 38.4 %	4129 ± 115.1 %
30	2425 ± 7.4 %	4788 ± 9.7 %	6639 ± 16.5 %	7036 ± 38.4 %
40	3203 ± 4.4 %	6319 ± 5.7 %	8661 ± 9.7%	9876 ± 19.3 %
50	3966 ± 3.1 %	7789 ± 3.9 %	10869 ± 6.3 %	12052 ± 12.9 %

Table 3: *Re* with uncertainty for impingement plate B

Suction Fan Setting (Hz)	Orifice Diameter (m)			
	0.02	0.03	0.04	0.05
	Re			
10	652 ± 115.06 %	null	null	null
20	1450 ± 23.1 %	2550 ± 38.42 %	2700 ± 115.06 %	null
30	2320 ± 9.03 %	3880 ± 16.55 %	4620 ± 38.42%	4350 ± 115.06 %
40	3080 ± 5.29 %	5270 ± 9.03 %	6500 ± 19.28%	7420 ± 38.42 %
50	3800 ± 3.69 %	6530 ± 6.01 %	7940 ± 12.92 %	8540 ± 28.84%

Table 4: *Re* with uncertainty for impingement plate C

Suction Fan Setting (Hz)	Orifice Diameter (m)			
	0.02	0.03	0.04	0.05
	Re			
10	614 ± 115.1 %	1409 ± 115.5 %	null	null
20	1608± 16.5 %	3106 ± 23.1 %	3591 ± 57.6 %	4129 ± 115.1 %
30	2425 ± 7.4 %	4586 ± 10.6 %	6154 ± 19.3 %	7036 ± 38.4 %
40	3203 ± 4.4 %	6168 ± 5.9 %	8661 ± 9.7%	9876 ± 19.3 %
50	3920 ± 3.2 %	7909 ± 3.8 %	10869 ± 6.3 %	12693 ± 11.6 %

Table 5: *Re* with uncertainty for impingement plate D

Suction Fan Setting (Hz)	Orifice Diameter (m)			
	0.02	0.03	0.04	0.05
	Re			
10	614 ± 115.1 %	1409 ± 115.5 %	null	null
20	1608 ± 16.5 %	3106 ± 23.1 %	4378 ± 38.4 %	4129 ± 115.1 %
30	2348 ± 7.8 %	4586 ± 10.6 %	6639 ± 16.5 %	7036 ± 38.4 %
40	3146 ± 4.7 %	6013 ± 6.2 %	8661 ± 9.7%	9032 ± 23.1 %
50	3873 ± 3.2 %	7543 ± 4.2 %	10582 ± 6.6 %	11374 ± 14.5 %

3.2. Thermochromic Liquid Crystal (TLC) calibration

The process of TLC calibration can be said as one of the most important part in determining the thermography of the transient liquid crystal. The calibration of TLC provides required and some additional information about the TLC that been used especially the color intensity-temperature relationship that been used to determine the heat transfer coefficient during the actual transient test.

Table 6: *Re* with uncertainty for impingement plate E

Suction Fan Setting (Hz)	Orifice Diameter (m)			
	0.02	0.03	0.04	0.05
	Re			
10	652 ± 115.06 %	1760 ± 115.06 %	null	null
20	1580 ± 19.28 %	2550 ± 38.41 %	2700 ± 115.06 %	null
30	2410 ± 8.41 %	4150 ± 14.51 %	5320 ± 28.84 %	4350 ± 115.06 %
40	3210 ± 4.91 %	5470 ± 8.41 %	7010 ± 16.55%	7420 ± 38.41 %
50	3960 ± 3.46 %	6840 ± 5.5 %	8760 ± 10.62 %	9530 ± 23.10 %

From the TLC calibration process, three relationships were obtained. The first one was the relationship between average intensity color play of TLC with total frames number, the seconds ones were the relationship between average color play intensity of TLC with the time and the last one was the relationship between the surface temperature with time. The first two relationship is obtained from the calibration video which contain the recorded color play of the TLC that been extracted into 25 framed per second. Then, the third relationship was obtained from the reading of T-type thermocouple which been place at the center of calibration plate that connected to data acquisition and to the personal computer. Figures 8, 9 and 10 shown all the relationships that been mention previously that obtained from the calibration raw data.

From the relationship between average intensity and frames number that been shown in Figure 8, there are two different peaks obtained from the total of 4000 frames of image that extracted from the captured calibration video. This relationship represents only the intensity of green color wave which was the most significant and dominant color play compared to red and blue color wave. Both these peaks in the figure represent different type of liquid crystal's activity. the first peak which from frame 500 to frame 1200 represent the heating process on the liquid crystal while the second peak which from frame 2400 to frame 3100 represent the cooling process on the liquid crystal.

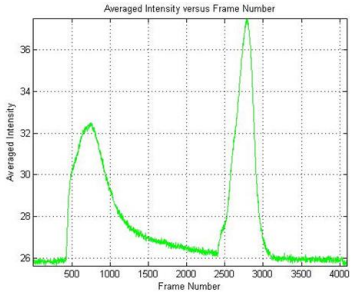


Fig. 8: Relationship between average intensity with frames number

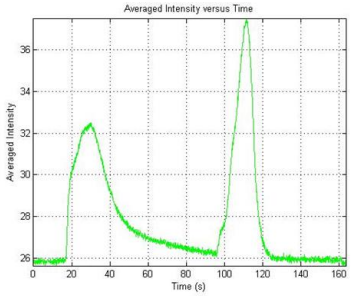


Fig. 9: Relationship between average color intensity with time

The recorded color play of the thermochromic liquid crystal in response of the temperature change was extracted into 25 frames per second. Therefore, the total frames will be divide with 25 and the time will be tally with the thermocouple time that been recorded by the data acquisition system. The average color intensity for Figure 9 will be similar as in Figure 8. These two figures summarized and validated the behavior of the liquid crystal. The TLC color play response to temperature changes start from colorless state to red, green and finally blue before turning colorless again because the temperature has exceeded the clearance point for the TLC. This color play pattern of TLC can be seen in Figure 8 at time around 19 second to 50 second which during the heating process. During cooling process activity, the TLC was exhibit hysteresis behavior which the color changes in reverse manner

from colorless, to blue green and finally red before becoming colorless again.

The level of intensity below 26 was indicating the state where there was no activity on the TLC which mean that the TLC did not reflecting any light into red, green or blue. In both Figures 8 and 9, average intensity been used instead a normal intensity is because the obtained intensity need to be averaged to eliminate the unwanted random variable noise from the extracted image [16].

The temperature reading of the thermocouple that obtained from the data acquisition was shown in Figure 10. However, Figure 10 only shown the heating process of the calibration test. From the figure, at time about 30 seconds, the surface temperature at the calibration plate was about 40℃. This temperature was the clearance temperature of the TLC where the green color intensity slowly turns colorless which was indicated by the intensity peak in both Figures 8 and 9.

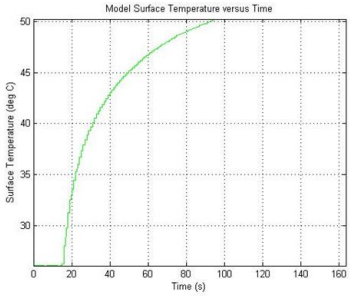


Fig. 10: Relationship between surface temperature and time

With these three relation that obtained, the forth relationship were obtain that also been generated by the calibration routine which is the relationship between the average intensity and surface temperature as shown in Figure 11. This relationship graph was obtained from the combination and matching process of the intensity history and the surface temperature of the calibration plate. However, since only heating process was needed, therefore the relationship only generated for the heating process part and the cooling process part was ignored.

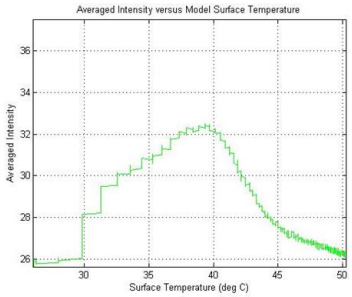


Fig. 11: Relationship between average intensity and surface temperature

The last relationship that been generated by the routine was the normalized average intensity curve which been shown in Figure 12. For this relationship, the average intensity was normalized because to rectify the variation of intensity for the next experiment where the lighting and the viewing condition may not always consistence every time the experiment been conducted due to human factor. This relationship would be used as reference information for the actual transient liquid crystal heat transfer experiment or also known as hot test.

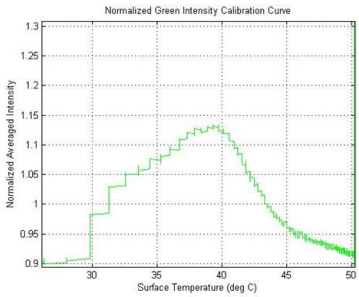


Fig. 12: Normalized average intensity calibration curve

Each result obtained from the experiment that been conduct were analyzed based on the output yield from the calibration analysis. The intensity-temperature histories were used as the benchmark for the experimental work result. The analyzing routine will search and compare the result and the intensity-temperature history to have the minimal error possibilities for each step in the analyzing process which involves combining the heat transfer coefficient and surface temperature histories, T_{bar} matching the intensity histories and generating the surface temperature histories. Basically, the analyzing process for the transient heat transfer experiment data involve MATLAB routine that have been developed earlier.

Basically, the analysis process of the transient heat transfer images consists of flow of steps that must be followed. First step involves a regression deduction process of the heat transfer coefficient and normalized temperature so that it compatible for the calculation of the possible surface temperature. From here, the relationship between heat transfer coefficient, normalized temperature and the surface temperature were compiled to form some experimental data libraries that been used for next step. Based on the color play of the TLC, green color intensity histories were generated for each pixel in the picture.

These experimental color intensity histories were compared with the calibrated color intensity and surface temperature histories which was the second step in the routine. This comparison allowed matching process between the experimental color intensity histories with the possible surface temperature based on the relationship that was obtained during the calibration analysis. Each surface temperature matched now contains possible combination of heat transfer coefficient and the normalized temperature. The data of each pixel was then combined to form map full of surface temperature, heat transfer coefficient and normalized temperature which was the fourth step.

The last step in the routine was to validate the result obtain from the previous steps. this was because the result from the previous step may subjected to be invalid and further filter could not be done as t will alter and lowering the heat transfer coefficient and surface temperature. Therefore, the last step in the routine will validate the heat transfer coefficient, surface temperature and normalized temperature from the previous step and compare the matching level between the experimental intensity histories with the calibration intensity history (ideal). Figure 13 shown a sample of the best possible matched intensity history which indicates that the most valid result. While Figure 14 shown a sample of the unsuitable matched intensity history due to the images noise during the extraction process or refection from the viewing angle which cause the data to be invalid to be choose.

3.3. Hot test

Hot test or transient heat transfer experiment test involving the multiple round jet impingement holes which consists of two different diameter configurations will be discussed into few main interests which are focusing on;

a. The effect of *Re*,
b. Impingement jet hole configuration

c. The effect of the present of small jet holes between the big/main jet holes on the heat transfer.

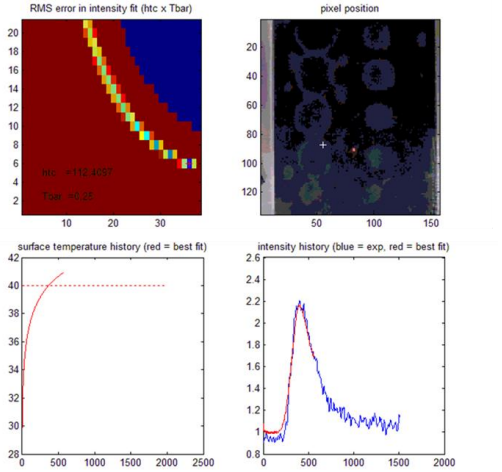


Fig. 13: Best matched intensity history for impingement plate A

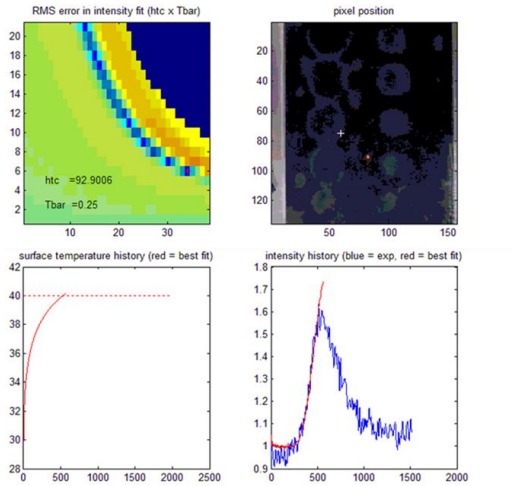


Fig. 14: Unsuitable matched intensity history for impingement plate A

Each impingement plate in this experiment with small hole consists of two different diameter of holes which was 10 mm and 5 mm diameter while the plate that without small holes has hole diameter of 10 mm. The reason behind these diameters selection is because big diameter holes has large mass flow rate which will contribute to higher local heat transfer while smaller holes has higher impingement air velocity which contribute to higher stagnation heat transfer [7].

Based on the MATLAB routine for transient heat transfer experiment that was mentioned previously, the result data obtained was shown in Figure 15. For each impingement plate that been analyzed the format of the figure data are similar.

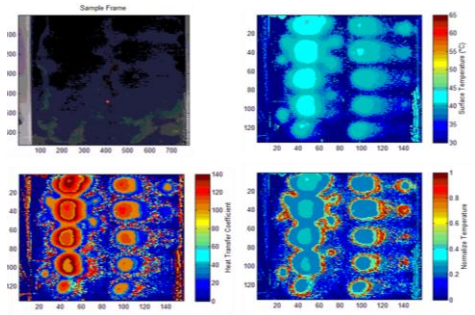


Fig. 15: Results from transient heat transfer MATLAB routine analysis for plate B, *Re* = 3966

In Figure 15, there are four sub-images which showing different information. On the upper left was the one of the sample extracted input images. Usually this image was the image when the heating process began. On the upper right image showed the resultant surface temperature on the target plate calculated analytically based on the heat transfer coefficient and normalized temperature that ware generated during TLC calibration process. The surface temperature map also been visualized from the best match of intensity history which compare between the experimental data and the calibration data. The corresponding heat transfer coefficient and normalized temperature were plotted in the lower left and right sub-image respectively. Only one figures of the result was shown for example purpose. Later in this chapter, only heat transfer coefficient data will be taken for analyses.

To confirm the values of the surface temperature, a thermocouple was located on the stagnation point of the target plate using impingement plate B. The surface temperature history for the stagnation point was shown in Figure 16 while the jet wall surface temperature is show in Figure 17. Through literatures, the temperature region around the stagnation point is slightly higher than the wall region. Based on the two figures below, this statement was validated. the temperature history logged that been show that the value of surface temperature at stagnation point was around 41 to 43 while the surface temperature for the jet wall region is around 39 to 41. Therefore, it was validated that at stagnation point the surface temperature is slightly higher than the jet wall region.

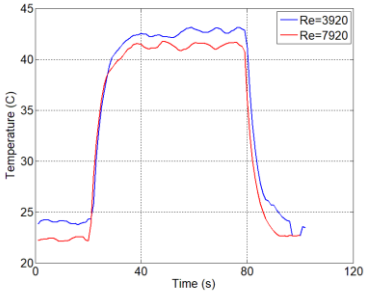


Fig. 16: Surface temperature history at the stagnation point

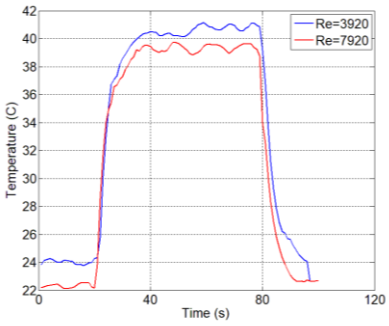


Fig. 17: Surface temperature history at the jet wall point

3.3.1. Rate of heat transferred across the plate surface.

For the rate of heat transfer across the target plate, it discussed based on the *Re* and the holes configuration.

For the effect of the *Re*, it shown on Figure 18a, as the *Re* increased, the rate of the heat transferred across the plate was faster compared to the one with low *Re* based on the red color region coverage on the figure. Based on the color bar, red was indicating the highest heat transfer coefficient while decreasing as the color goes from red to blue. This meant that as the *Re* increased, the red color region was larger (high heat transfer coefficient) while for lower *Re*, the red color coverage was not as bigger as the one on the high *Re*. This shown that the more heat been transferred to the surface at higher *Re* compared to for the one with low *Re*. This was because as the *Re* was high, the mass flow rate was also high. This cause the heated air been pass through the holes were more compared to the low *Re*. However, this was with the present of the small holes between the main big holes which contribute to the uniformity of the air flow. As compared with the absent of the

small holes (Figure 18b), the rate of heat transferred across the plate was lower as the *Re* went up which showing the opposite observation that was made from the one with the present of the small holes. As been stated previously, this may be caused by the uniformity of the air flow passing through the holes that was better as the small holes been placed between the main big holes.

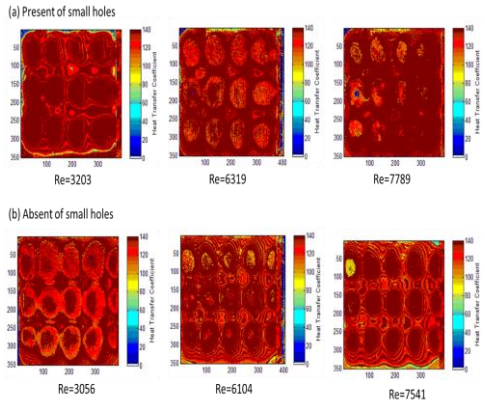


Fig. 18: Effect of *Re* on the heat transfer across the plate for inline holes configuration

For staged holes configuration however, the observation was reversed. It been observed that for the plate that has smaller holes (Figure 19a) had low rate of heat transfer across the target plate as the *Re* increased, while for the plate that does not had smaller holes (Figure 19b) gave higher rate of heat transfer across the target plate as the *Re* increased. This may be due to the cross flow affect that occur between the holes. Another explanation that can be stated based on the observation was that, as the *Re* increased, the end of the jet impingement potential core moved slowly toward the target plate. This behavior could closely relate to Gillespie *et al*. [17] which explained that due to the flow separation, the ejected impingement jet would experience a decreasing in heat transfer process. Therefore, further distance between the jet plate and target plate would be needed. This was explained by Goldstein *et al*. [18] that stated that further distance would be needed for higher *Re* as the jet impingement potential core was no fully developed when it reaches the target plate. The potential core must be fully developed to get higher heat transferred to the surface. Under developed core caused same heat was not spread evenly and over developed core cause some heat lost.

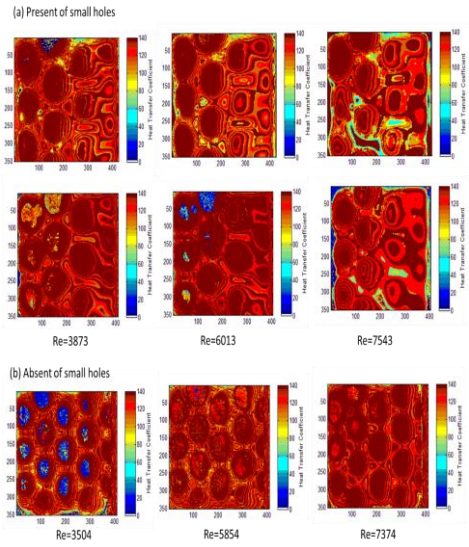
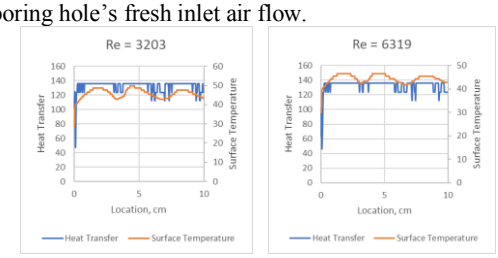


Fig. 19: Effect of *Re* on the heat transfer across the plate for staged holes configuration

3.3.2. Cross flow effect on the heat transfer

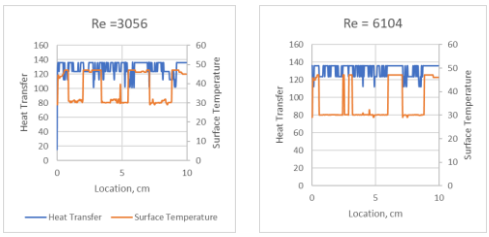
As been stated previously, the heat transfer across the target plate may be affected by the cross flow that form between the holes. The formation of the cross flow was due to the air that deflected to the side and disturbing the incoming fresh air that pass through the holes. It may cause the reduction of heated new income air temperature. This was because the deflected air temperature was lower due to the fact some of the heat has been transferred to the target surface and when it in contact with the fresh income air, it will somehow have absorbed some of the heat form the fresh income air. This cause the temperature of the fresh incoming air reduced which reduced level of heat been transfer to the target surface

As for inline holes configuration as shown in Figure 20 and 21, the present of the small holes improve the value of the surface temperature across the target plate surface as *Re* increased when compared with the one that does not have small holes which reduction of surface temperature occurred as the *Re* increased. This was because of the air that passes through the small holes act as the wall that reduce some of the air from the main big holes that defected after impinged the target surface which will disturb the neighboring hole's fresh inlet air flow.



(a) (b)

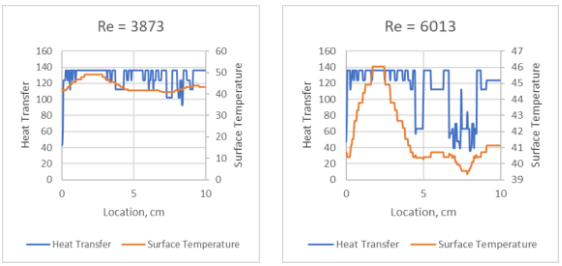
Fig. 20: Inline holes configuration with small holes



(a) (b)

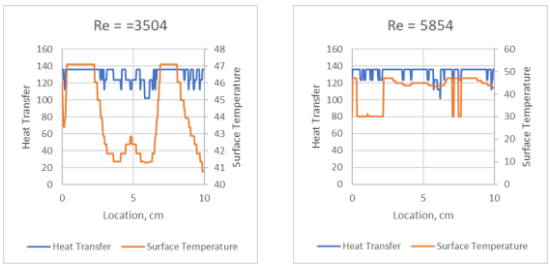
Fig. 21: Inline holes configuration without small holes

As for the staged holes configuration (Figure 22 and 23), different observation has been obtained. It shows that, with the presence of small holes, the surface temperature across the target plate surface was lower as compared with the one with the absent of the small holes where the surface temperature across the target plate were at the better level. The explanation that can be made is that, the positioning of the small holes in between the main big holes does not giving a desired effect like the one occurred for the inline configuration. The placement of the small holes might be too close to the big holes which cause the air were not able to be passed through it caused the air had higher tendency to only pass through the big hole. Another explanation that could be made is, since position of the small holes and the big holes is too closes which causes the air from the small holes cause the cross-flow effect. In other words, the distance between the small and main big holes also contribute to the occurrence or strength of the cross flow between the holes. The plate without the smaller holes show higher surface temperature compared to the one with the small hole was because of spacing between the holes that more optimum and less formation of cross flow. This is explained by Taslim & Rosso [19] and Yong *et al*. [20] that obtain similar observation. According to them, due to the small spacing between holes, the formation of cross flow was weakened the penetration of the impingement air. The crossflow will cause the reduction of new inlet hot fresh air temperature before impinging the target plate surface.



(a) (b)

Fig. 22: Staged holes configuration with small holes



(a) (b)

Fig. 23: Staged holes configuration without small holes

Based on the figures above, which show the result for both inline and staged configuration with or without the presence of small holes, it can be said that inline configuration with the presence of the small holes gives a better performance as it has better surface temperature across the target plate and more consistent heat transfer compared to the other holes configuration. As explained earlier, with the presence of small holes, it helps to uniform the heated air flow across target plate and act as the wall that reduce the effect of the cross flow on the neighboring big holes.

4. Conclusions

The study on the effect of different holes configuration and varied *Re* was observed and discussed as detail as possible.

1. The hypothesis that been made during the earlier stage of the study which was higher *Re* will have higher heat transfer across the target plate was not entirely true. Logically, if *Re* is higher, mass flow rate was higher. However, in this study it occurs oppositely for some test plate. The heat transfer coefficient was lower at high *Re*. This was because the jet impingement core was not fully developed. Therefore, bigger spacing between the jet plate and the target plate needed to ensure that the impingement core was fully developed and coincide with the target plate surface.

2. Besides that, staged configuration with the present of small in between the main big impingement jet holes that were stated will yield higher heat transfer coefficient compared to another hole configuration was not either wrong or right. This was because it been observed that the heat transfer performance for inline holes configuration with the present of small holes was better than the other configuration. In addition, it also can be concluded that with the present of small holes, the heat transfer performance across the target pate is better as compared with the one without the small holes.

3. Finally, based on the overall observation that been made, it can be concluded that the design parameters were found to be not a stand-alone criterion in determining the heat transfer coefficient. Based on the pre-established design parameter, only certain combination of parameter will yield higher level of heat transfer coefficient and *Nu* distribution. Higher *Re* did not always give higher heat transfer coefficient. In fact, combination of holes diameter, hole to hole spacing, and *Re* that been made in a right way were required to enhance higher level of heat transfer across the surface of interest.

Acknowledgement

The authors would like to thank the Ministry of Higher Education for their support through Fundamental Research Grant Scheme TK05/UPM/02/7 (vot. No. 5524896). Special gratitude to Mr Mohd Nasir Johari Assistant Engineer at the Propulsion Laboratory Universiti Putra Malaysia for the technical assistance.

References

[1] Mohd Saiah H (2006), Heat transfer measurements on flat plate surface film cooling. Department of Aerospace Engineering, Universiti Putra Malaysia, Malaysia.
[2] Ndao S, Peles Y & Jensen MK (2014), Effects of pin fin shape and configuration on the single-phase heat transfer characteristics of jet impingement on micro pin fins. *International Journal of Heat and Mass Transfer* 70, 856-863.
[3] Fechter S, Terzis A, Ott P, Weigand B, Von Wolfersdorf J & Cochet M (2013), Experimental and numerical investigation of narrow impingement cooling channels. *International Journal of Heat and Mass Transfer* 67, 1208-1219.
[4] Liao G, Wang X, Li J & Zhang F (2014), A numerical comparison of thermal performance of in-line pinefins in a wedge duct with three kinds of coolant. *International Journal Heat Mass Transfer* 77
[5] Hollworth BR & Dagan L (1980), Arrays of impinging jets with spent fluid removal through vent holes on the target surface—Part 1: Average heat transfer. *Journal of Engineering for Power* 102(4), 994.
[6] Liu HY, Liu SL, Qiang QF & Liu CL (2013), Aerodynamic investigation of impingement cooling in a confined channel with staggered jet array arrangement. *Experimental Thermal and Fluid Science* 48, 184-197.
[7] Singh D, Premachandran B, Kohli KS & Kim SJS (2013), Experimental and numerical investigation of jet impingement cooling of a circular cylinder. *International Journal of Heat and Mass Transfer* 60, 672-688.
[8] Yang Y, Wang Y & Hsu J (2015), Numerical thermal analysis and optimization of a water jet impingement cooling with VOF two-phase approach. *International Communications in Heat and Mass Transfer* 68, 162-171.
[9] BS1042 measurement of fluid flow in closed conduit. British Standard 1981.
[10] Abdullah N, Abu Talib AR, Jaafar A, Mohd Saiah H & Mohd Salleh M (2009), Film thickness effects on calibrations of a narrowband thermochromic liquid crystal. *Experimental Thermal and Fluid Science* 33, 561-578.
[11] Holman J (1997), *Heat Transfer*, New York: McGraw-Hill.
[12] Bai Y (2014), Thermal conductivity model with non-constant boundary condition in one-dimensional semi-infinite case. *Applied Mechanics and Materials* 685, 254-258.
[13] Suryantari R (2015), Linearization of hue value on the surface of thermochromic liquid crystal with variation of temperature. *Indonesian Journal of Applied Physics* 5(01), 2015.
[14] Abdullah N, Talib AR, Jaafar AA, Salleh MA & Chong WT (2010), The basics and issues of thermochromic liquid crystal calibrations. *Experimental Thermal and Fluid Science* 34(8), 1089-1121.
[15] *Agilent 34970A Data Acquisition / Switch Unit user manual*. Technologies Agilent, 2007.
[16] Abdullah N, Abu Talib AR, Jaafar AA, Mohd Saiah H & Mohd Salleh MA (2007), Development of a graphical user interface (GUI) for processing images in transient thermochromic liquid crystal calibration. AEROTECH-II.
[17] Gillespie DRH, Wang Z, Ireland PT & Kohler ST (1998), Full surface local heat transfer coefficient measurements in a model of an integrally cast impingement cooling geometry. *Journal of Turbomachinery* 120, 92-99.
[18] Goldstein RJ, Behbahani AI & Heppelmann KK (1986), Streamwise distribution of the recovery factor and the local heat transfer coefficient to an impinging circular air jet. *International Journal of Heat and Mass Transfer* 29(8), 1227-1235.
[19] Taslim ME & Rosso N (2012), Experimental/numerical study of multiple rows of confined jet impingement normal to a surface at close distances. *Heat Transfer*
[20] Yong S, Jing-Zhou Z & Gong-Nan X (2015), Convective heat transfer for multiple rows of impinging air jets with small jet-to-jet spacing in a semi-confined channel. *International Journal of Heat and Mass Transfer* 86, 832-842.